

# Numerical Study on Aging Dynamics in Ising Spin-Glass Models: Temperature-Change Protocols

Tatsuo KOMORI\*, Hajime YOSHINO\*\* and Hajime TAKAYAMA\*\*\*

*Institute for Solid State Physics, the University of Tokyo, 7-22-1 Roppongi, Minato-ku, Tokyo 106-8666*

(Received February 5, 2020)

By means of Monte Carlo simulations on the three-dimensional Ising spin-glass model, we have studied aging phenomena with various temperature( $T$ )-change protocols. Particularly, a  $T$ -shift protocol, in which a system is first quenched to and aged for a period  $t_{w1}$  at a temperature  $T_1$ , and subsequently aged at a new temperature  $T_2$  is closely investigated. Most importantly, the mean size of domains, which is extracted from the replica-overlap function, was found to grow monotonically without any appreciable decrease by the  $T$ -change. We also found the relaxation of energy density and spin auto-correlation function during the  $T$ -shift process can be explained within the following picture: the dynamics finally crossovers to an isothermal aging of  $T_2$  at around  $t_2 \simeq t_{w1}^{(\text{eff})}$  after the  $T$ -change, where  $t_{w1}^{(\text{eff})}$  is an effective waiting time related with  $t_{w1}$ , but in the transient regime  $t_2 \lesssim t_{w1}^{(\text{eff})}$ , adjustment of the population of thermally active droplets from that at  $T_1$  to  $T_2$  takes place very slowly. Implications of the results on aging phenomena in other  $T$ -change protocols such as  $T$ -cycling and continuous  $T$ -change with an intermittent stop observed by simulations as well as experiments are discussed.

KEYWORDS: spin glass, slow dynamics, aging, droplet theory

## §1. Introduction

Aging phenomena in spin glasses have been extensively studied in recent years. Experimentally, many elaborated protocols have been adopted to reveal various aspects of the phenomena.<sup>1, 2, 3)</sup> Theoretically, on the other hand, many ideas and models on spin glasses and related systems have been proposed and examined to get a proper understanding of aging dynamics in such glassy systems.<sup>4, 5)</sup> On the side of numerical study, a number of simulations, which could account for qualitative features of the aging effects, have been performed.<sup>6, 7, 8)</sup> In spite of the enormous efforts, however, a unified picture of aging dynamics in spin glasses has not been established yet. The difficulty is directly connected to nature of the low-temperature spin-glass (SG) phase which has been a controversial issue since more than a decade ago.

Among simulational results on the short-ranged Ising SG models, of particular importance is the growth of a mean domain size which is observed through the replica-overlap function,  $G(r, t)$ , in isothermal aging after a system is quenched instantaneously from temperature above its SG transition temperature  $T_c$  to  $T$  below  $T_c$ .<sup>9, 10, 11, 12)</sup> The function  $G(r, t)$  is defined as

$$G(r, t) = \frac{1}{N} \sum_{i=1}^N \left[ S_i^{(\alpha)}(t) S_i^{(\beta)}(t) S_{i+r}^{(\alpha)}(t) S_{i+r}^{(\beta)}(t) \right]_{\text{av}}, \quad (1.1)$$

where  $\alpha$  and  $\beta$  are indices of two replicas which have dif-

ferent random spin configurations at  $t = 0$  (an instant of the quench), and are independently updated. Its correlation length  $R_T(t)$  is found to grow almost in a power-law in the case of 3 dimensional (3D) models,<sup>10, 11, 12)</sup>

$$R_T(t) \sim L_0(t/\tau_0)^{1/z(T)}, \quad (1.2)$$

where  $L_0$  and  $\tau_0$  are certain characteristic units of length and time, respectively, and the exponent  $1/z(T)$  depends on  $T$ . In our previous work,<sup>12)</sup> hereafter referred to as I, we obtained

$$1/z(T) \simeq 0.17T, \quad (1.3)$$

at  $T < 0.7J$  for the Gaussian model with zero mean and variance of interactions  $J$ . More precisely, it can be also fitted to a logarithmic functional form written as  $R_T(t) \simeq R_0 + b(\ln t)^{1/\psi}$  with  $R_0, b$  and  $\psi$  being constants.<sup>9, 10, 13)</sup> This ambiguity is attributed to the insufficiency of the time window of simulations by presently available computers. Although there remains such an ambiguity in the explicit growth form of  $R_T(t)$ , we can naturally regard  $R_T(t)$  as a characteristic length scale of the SG ordering in aging dynamics, i.e., a mean distance of domain walls separating different pure states.

It is natural to ask to what extent the mean domain size  $R_T(t)$  is related to aging behaviours observed in various quantities simulated. The droplet theory,<sup>14, 15, 16, 17)</sup> particularly the one proposed by Fisher and Huse<sup>17)</sup> contains scaling ansatz which relate various quantities to the characteristic length scales such as  $R_T(t)$  mentioned above. We have been numerically studying aging phenomena in the 3D Ising SG model to clarify the validity of the ansatz.<sup>12, 13, 18)</sup>

Experimentally, various interesting phenomena have

\* Present address: Hydrographic Department, Maritime Safety Agency, 5-3-1 Tsukiji, Chuo-ku, Tokyo 104-0045

\*\* E-mail: yhajime@ginnan.issp.u-tokyo.ac.jp

\*\*\* E-mail: takayama@issp.u-tokyo.ac.jp

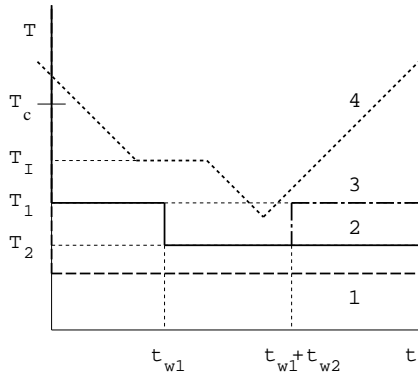


Fig. 1. Schedules of  $T$ -change in some experimental protocols of aging: 1) isothermal, 2)  $T$ -shift, 3)  $T$ -cycle, and 4) continuous  $T$ -change with an intermittent stop.

been also observed in aging processes other than the isothermal one. They are  $T$ -shift,  $T$ -cycling, and continuous  $T$ -change with an intermittent stop(s) protocols whose schedules of  $T$ -change are schematically shown in Fig. 1. The ac susceptibility has been continuously measured through these  $T$ -changes. In the case of a negative  $T$ -shift process with  $\Delta T \equiv T_2 - T_1 < 0$  in Fig. 1 and with a magnitude  $|\Delta T|$  larger than a certain value, the ac susceptibility is observed to increase discontinuously just after  $t = t_{w1}$  and then to relax again.<sup>19, 20, 21)</sup> Its behaviour looks as if the system restarts aging by the  $T$ -shift at  $t = t_{w1}$  forgetting its thermal history before  $t_{w1}$ . It is called the *rejuvenation*, or *chaos effect*. Furthermore when the temperature is turned back to  $T_1$  at  $t = t_{w1} + t_{w2}$  ( $T$ -cycling protocol), the value of the ac susceptibility returns to that on the isothermal aging curve of  $T_1$  at almost  $t = t_{w1}$ , and then relaxes along the curve. This behaviour indicates that the system in fact remembers its history before  $t_{w1}$ , and is called the *memory effect*. Similar coexistence of the paradoxical phenomena, rejuvenation and memory effect, has been recently observed also in a continuous  $T$ -change with an intermittent stop(s).<sup>22, 23)</sup> These experimental findings have stimulated theoretical interest.<sup>5)</sup>

The main purpose of the present paper is to investigate aging phenomena in various  $T$ -change protocols by simulations on the 3D Gaussian Ising SG model.<sup>24)</sup> We concentrated mostly on the  $T$ -shift process, which is the most fundamental among the various  $T$ -change protocols, since the latter are considered as certain combinations of the former. We investigated the time evolution of the mean domain size and the relaxation of the energy density and the spin auto-correlation function during the  $T$ -shift process.

We have found, within the time window of our simulations, the following characteristic features of the aging dynamics. i) The mean domain size  $R_{[T_2, T_1]}(t; t_{w1})$  in the  $T$ -shift process (see Fig. 1), with either a negative or positive  $\Delta T$ , does continue to grow. Here and hereafter  $t$  is a time measured from the first quench from above  $T_c$  to  $T_1$ ,  $t_2 = t - t_{w1}$  a period that the system ages at  $T = T_2$  after the  $T$ -shift at  $t = t_{w1}$ . ii) The time evolution of the energy density and the spin auto-correlation func-

tion is related with the mean domain size  $R_{[T_2, T_1]}(t; t_{w1})$  at sufficiently long time scales after the  $T$ -shift by the scaling relations which are the same as isothermal aging. iii) However, there is a transient time regime after the  $T$ -shift where there is extra contribution to the relaxations. Interestingly, the extra contribution also shows very slow, non-exponential relaxation. We interpret the latter as not due to the chaos effect predicted by the droplet theory<sup>16, 17)</sup> but as due to adjustment of the population of droplet excitations within each domain.

The memory effect observed experimentally is easily interpreted from the above-mentioned scenario, namely, it is attributed to the persistence of domains in a  $T$ -shift process. It is not yet conclusive, however, whether nature of the transient regime in the scenario is common to phenomena observed experimentally just after a  $T$ -shift. In this respect, the recent work on aging in the ferromagnetic fine particles system (FFPS) done by Mamiya *et al.*<sup>25)</sup> is of quite interest, since the time window of their observation in unit of the microscopic time ( $\sim 10^{-3}$  sec for this system<sup>26)</sup>) is rather closer to that of our simulations. Indeed, they have observed  $T$ -shift aging phenomena which can be well interpreted by our scenario. It seems, however, that the scenario is hard to explain the rejuvenation, or chaos effect observed experimentally in ordinary spin glasses,<sup>19, 21, 27, 28)</sup> whose microscopic time is of the order of  $10^{-13}$  sec.

The present paper is organized as follows. In the next section we briefly review the scaling properties of isothermal aging derived from the droplet theory, add further comments on them, and present the scenario on the  $T$ -shift process. In §3 we present the results of our simulations on various aspects of the  $T$ -shift, as well as the  $T$ -cycling and continuous  $T$ -change processes. In the final section implications of the results with the experimental observations are discussed.

## §2. Phenomenological Picture

### 2.1 Scaling properties of isothermal aging

Here we briefly review the scaling properties of isothermal aging derived by the droplet theory<sup>17, 16)</sup> due to Fisher and Huse (FH). In an isothermal aging process a system is quenched from above  $T_c$  to temperature  $T$  below  $T_c$ . At waiting time  $t_w$  after the quench, there are domain walls separating different pure states of the SG phase at a typical distance  $R_T(t_w)$  from each other. The distance  $R_T(t_w)$  can be measured in simulations for instance through the replica overlap function defined in eq.(1.1).

Except for places where the domain walls run, the bulk of the system is essentially in equilibrium. An important subtle feature inside the domains of a spin glass is that there can be large scale thermal fluctuations due to droplet excitations. In ideal equilibrium, a droplet excitation can be defined as a global flip from a ground state of a droplet (cluster) of spins within a distance  $L/2$  from a certain given site  $i$ .<sup>16)</sup> The latter can be considered as a simple two-state system with a free-energy excitation gap  $F_L(i)$  and a barrier energy  $B_L(i)$  of a thermal activation process.

The typical value  $F_L^{\text{typ}}$  of the gap  $F_L(i)$  scales as,

$$F_L^{\text{typ}} \sim \Upsilon(L/L_0)^\theta, \quad (2.1)$$

where  $\Upsilon$  is the stiffness constant of domain walls on the boundary of the droplet. The gap is however broadly distributed and its distribution function  $\rho_L(F)$  is considered to follow the scaling form,

$$\rho_L(F) = \frac{1}{F_L^{\text{typ}}} \tilde{\rho} \left( \frac{F}{F_L^{\text{typ}}} \right). \quad (2.2)$$

A very important property of the scaling function  $\tilde{\rho}(x)$  is that it has finite intensity at  $x = 0$ ,  $\tilde{\rho}(0) > 0$ , which allows large scale droplet excitations even at very low temperatures. The probability to have a thermally active droplet at a very low temperature  $T$  is given by

$$p(L; T) \sim \frac{k_B T}{\Upsilon(L/L_0)^\theta} \tilde{\rho}(0). \quad (2.3)$$

The latter feature yields equilibrium properties which make spin glasses distinctly different from simple ferromagnets.<sup>16)</sup>

The relaxation time of a droplet of size  $L$  centered at site  $i$  is given by the Arrhenius law

$$\tau_L(i) = \tau_0 \exp \left( \frac{B_L(i)}{k_B T} \right), \quad (2.4)$$

where  $B_L(i)$  is the energy barrier of the droplet. The typical value  $B_L^{\text{typ}}$  of the energy barrier  $B_L(i)$  scales as,

$$B_L^{\text{typ}} \sim \Delta(L/L_0)^\psi, \quad (2.5)$$

where  $\Delta$  is a characteristic unit for energy barriers associated with thermal activation of droplet excitations, and the exponent  $\psi$  satisfies  $\theta \leq \psi \leq d - 1$ .

In the droplet theory, it is assumed that the growth of domains is also governed by droplet excitations. An obvious but very important consequence of eqs.(2.4) and (2.5) is that dynamical processes, including both the domain growth and droplet excitations, at different length scales are extremely widely separated.<sup>5)</sup> Hence within a time scale of small scale processes, large scale processes look as if they are almost frozen.

In isothermal aging, for example, the relaxation of the excessive energy per spin  $\delta e_T(t)$  with respect to the equilibrium value is expected to follow the scaling form as,

$$\delta e_T(t) \sim \tilde{\Upsilon}(R_T(t)/L_0)^\theta / (R_T(t)/L_0)^d, \quad (2.6)$$

where  $\tilde{\Upsilon}$  is a characteristic energy scale, and  $d$  is the dimension of space which is 3 here. This scaling form was confirmed, in our previous work I, with the energy exponent  $\theta = 0.20 \pm 0.03$  which agrees with the result of the defect energy analysis at  $T = 0$ .<sup>29)</sup>

The droplet theory also predicts important scaling properties of the spin auto-correlation function,

$$C_T(\tau; t_w) = \overline{\langle S_i(\tau + t_w) S_i(t_w) \rangle}, \quad (2.7)$$

in isothermal aging. Here the over-line denotes the averages over sites and different realizations of interactions (samples), and the bracket denotes the average over thermal noises. In the so-called quasi-equilibrium regime defined by  $\tau \ll t_w$ , the typical size  $L_T(\tau)$  of droplet exci-

tations which take place in the time scale of  $\tau$  is much smaller than the typical separation  $R_T(t_w)$  of domain walls present after the waiting time  $t_w$ . For this situation the droplet theory introduces a phenomenological concept called *effective stiffness* which characterizes a reduction of the excitation gap of small scale droplets due to the presence of the domain walls. The latter yields  $t_w$ -dependence of  $C_T(\tau; t_w)$  which is written in terms of  $R_T(t_w)$  and  $L_T(\tau)$  as the following:

$$1 - C_T(\tau; t_w) = \Delta C_T(\tau; t_w) + \alpha_T(\tau), \quad (2.8)$$

with

$$\alpha_T(\tau) = 1 - C_T^{(\text{eq})}(\tau), \quad (2.9)$$

and

$$\Delta C_T(\tau; t_w) \sim \tilde{\rho}(0) \frac{T}{\Upsilon} \left( \frac{L_0}{L_T(\tau)} \right)^\theta \left( \frac{L_T(\tau)}{R_T(t_w)} \right)^{d-\theta}. \quad (2.10)$$

Then the zero field cooled susceptibility  $\chi_{\text{ZFC};T}(\tau; t_w)$  which is often observed by experiments should also be understood within the same ansatz since the fluctuation-dissipation theorem (FDT)

$$\chi_{\text{ZFC};T}(\tau; t_w) \simeq \frac{1}{T} [1 - C_T(\tau; t_w)] \equiv \tilde{\chi}_T(\tau; t_w). \quad (2.11)$$

holds in the quasi-equilibrium regime. The FDT has been tested and confirmed by the careful experiments<sup>30,31)</sup> even in the presence of weak violation of the time translational invariance.

## 2.2 Further comments on isothermal aging

In our previous work,<sup>13)</sup> hereafter referred to as II, we confirmed the scaling ansatz on  $C_T(\tau; t_w)$  described in the previous subsection. Here, we first make the comment that  $\chi_{\text{ZFC};T}(\tau; t_w)$  experimentally observed and analyzed through eq.(2.11) also follow the scaling ansatz.

In Fig. 2, for example, we plot  $\chi_{\text{ZFC};T}(\tau; t_w)$  of a Ag:Mn 2.6at% spin glass against  $t_w/\tau$ . The latter is evaluated from  $m_{\text{TRM};T}(\tau; t_w)$  measured by the Saclay group<sup>1)</sup> as  $\chi_{\text{ZFC};T}(\tau; t_w) = [m_{\text{FC};T} - m_{\text{TRM};T}(\tau; t_w)]/h$  with  $m_{\text{FC};T}$  being the field-cooled magnetization under a field of strength  $h$ . The data for different  $\tau$ 's lie on a universal curve when they are vertically shifted by suitable amounts depending on  $\tau$  as shown in the inset of the figure. The feature is quite similar to  $1 - C_T(\tau; t_w)$  analyzed in II. [Note that the factor  $(L_0/L_T(\tau))^\theta$  is practically constant in eq.(2.10) since  $\theta$  is much smaller than  $d - \theta$ , as was the case of  $1 - C_T(\tau; t_w)$  in II.] This indicates that  $\chi_{\text{ZFC};T}(\tau; t_w)$ , via eq.(2.11), follows the scaling forms eqs.(2.8), (2.9) and (2.10) as well. The values of the exponents  $(d - \theta)/z(T)$  and  $\theta/z(T)$  turn out to agree roughly with the estimates using  $\theta$  and  $1/z(T) \simeq 0.18(T/T_c)$ , i.e., eq.(1.3) with  $T_c = 0.95 \pm 0.04$ ,<sup>32)</sup> extracted from our analysis in II. However, such semi-quantitative agreement is lost for the data at temperatures closer to  $T_c$ .

An intriguing point is that the above result suggests that  $R_T(t)$  in the time scale of experiments is also compatible with the estimate from our simulations. In this context it is worth pointing out that Joh *et al.*<sup>33)</sup> have recently extracted  $R_T(t)$  of Cu:Mn 6at% and

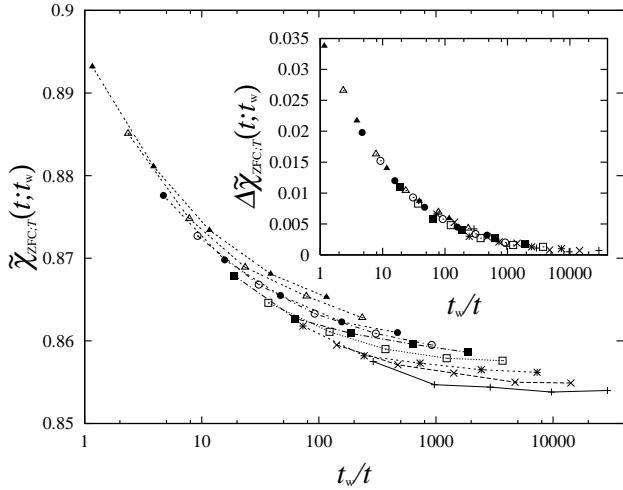


Fig. 2.  $\chi_{ZFC;T}(\tau; t_w)$  of a AgMn spin glass<sup>1)</sup> at  $T/T_c = 0.87$  for fixed  $\tau$ 's plotted against  $t_w/\tau$ ;  $\tau = 1, 2, 4, 8, \dots, 256$  sec from bottom to top and  $t_w = 300, 1000, 3000, 10000, 30000$  sec. In the inset the scaling behaviour of  $\Delta\chi_{ZFC;T}(\tau; t_w)$  corresponding to eq.(2.10) is demonstrated.

$\text{CdCr}_{1.7}\text{In}_{0.3}\text{S}_4$  spin glasses from the thermoremanent magnetization (TRM). The growth law they have obtained turns out to agree with the simulational result of eqs.(1.2) and (1.3) even quantitatively. The estimated  $R_T(t)$  with  $t$  of the order of laboratory time is at most only several tens of lattice distances. However, the experimental studies on the isothermal aging dynamics so far reported have not converged to a unified picture yet as we discussed in II.

Another comment is related to the characteristic length and time scales,  $L_0$  and  $\tau_0$  in eq.(1.2), which we did not fix explicitly in II. According to the droplet theory,<sup>16)</sup> they are some microscopic scales at lower temperatures, but near below  $T_c$  they are expected to crossover to the SG coherence length  $\xi_-$  and the corresponding critical relaxation time, respectively. Indeed, Hukushima *et al.*<sup>34)</sup> have found recently such a crossover behaviour in aging dynamics in the 4D  $\pm J$  Ising SG model. A similar analysis on the present 3D model certainly has to be done, which may clarify the disagreement between the experimental and simulational results close to  $T_c$  mentioned just above. Furthermore, as suggested in,<sup>34)</sup> it may also provide a useful key to resolve the apparent ambiguity of the growth law mentioned previously.

### 2.3 $T$ -shift process within overlap-length

Now let us consider the  $T$ -shift process. After a system is first quenched from above  $T_c$  to a temperature  $T_1$  below  $T_c$ , domains of different pure states grow up. Their mean size reaches to  $R_{T_1}(t_w)$  after a given waiting time  $t = t_w$ . After the temperature is changed at  $t = t_w$  to a new temperature  $T_2$ , we expect the domains continue to grow but with a rate specific to the new temperature  $T_2$  (see eq.(3.1) below). It can be said that, at the instant of the  $T$ -shift, the system is aged as if it is aged for the effective waiting time  $t_w^{(\text{eff})}$  by isothermal aging

at  $T_2$ , where  $t_w^{(\text{eff})}$  is determined by

$$R_{T_1}(t_w) \simeq R_{T_2}(t_w^{(\text{eff})}), \quad (2.12)$$

with  $R_T(t)$  being the growth law of the mean domain size in isothermal aging at  $T$ .

Another important process which must take place after the  $T$ -shift is adjustment of the population of thermally active droplets within the domain. Since the equilibrium population is proportional to  $T$  as given in eq.(2.3), there must be a change of the population of an amount proportional to  $\Delta T = T_2 - T_1$  at each length scale  $L$ . It is emphasized that this process itself is intrinsically very slow since adjustment of the droplets takes place only by activation processes described by eqs.(2.4) and (2.5). Thus we naturally expect that there is a new characteristic length  $L_{[T_2, T_1]}(t_2, t_w)$  which slowly grows after the  $T$ -shift such that the population of droplets smaller than  $L_{[T_2, T_1]}(t_2, t_w)$  is equilibrated to the new temperature  $T_2$ . However, the population of droplets larger than  $L_{[T_2, T_1]}(t_2, t_w)$  is still equilibrated with respect to the old temperature  $T_1$ . We call the characteristic length  $L_{[T_2, T_1]}(t_2, t_w)$  as a size of *quasi-domains*.

The growth law of  $L_{[T_2, T_1]}(t_2, t_w)$  is expected to be the same as the domain. When the system ages at  $T_2$  for a period about  $t_w^{(\text{eff})}$  defined by eq.(2.12),  $L_{[T_2, T_1]}(t_2, t_w)$  catches up  $R_{[T_2, T_1]}(t; t_w)$  and the quasi-domains merge into domains in isothermal aging at  $T_2$ . Thus at large time scales  $t_2 \gtrsim t_w^{(\text{eff})}$ , aging becomes essentially the same as isothermal aging at  $T_2$ . The time range  $t_2 \lesssim t_w^{(\text{eff})}$ , on the other hand, is regarded as a transient regime where adjustment of the population of droplets are taking place.

In the above argument we implicitly assumed that equilibrium states at different temperatures are the same except for the change of the population of droplets eq.(2.3). It should be remarked that the assumption makes sense only for length scales smaller than the so-called overlap length  $l_{\Delta T}$ .<sup>16,35)</sup> It is predicted that equilibrium states at different nearby temperatures  $T_1$  and  $T_2$  differ from each other at length scales larger than this length  $l_{\Delta T}$ . This aspect is called *chaotic* nature of the SG phase.<sup>35)</sup> The overlap length  $l_{\Delta T}$  is expected to diverge when  $\Delta T = T_2 - T_1 \rightarrow 0$  as

$$l_{\Delta T} \sim L_0 \left( \frac{\Upsilon^{3/2}}{T^{1/2} |\Delta T|} \right)^{2/(d_s - 2\theta)}, \quad (2.13)$$

where,  $\theta$  is the exponent in eq.(2.1) and  $d_s$  the fractal dimension of surface of the droplets.

## §3. Results of Simulations

### 3.1 Model and method

We have carried out MC simulations on various aging processes in the same 3D Ising SG model as in our previous works, i.e., the one with Gaussian nearest-neighbor interactions with mean zero and variance  $J = 1$ , and with  $T_c = 0.95 \pm 0.04$ .<sup>32)</sup> The heat-bath MC method we use here is also the same as in I and II. The data we will discuss below are obtained mostly at  $T = 0.6 \sim 0.8$  in systems with linear size  $L_s = 24$  averaged over a few hundreds samples with one MC run for each sample. In I, it was confirmed that finite size effects do not appear

for these parameters within our time window ( $\lesssim 2 \times 10^5$  MCS).

### 3.2 SG coherence length — domain growth

Let us begin with time evolution of  $R_{[T_2, T_1]}(t; t_{w1})$ , a mean domain size in a negative  $T$ -shift protocol with  $\Delta T = T_2 - T_1 < 0$  (see Fig. 1). The simulated results with  $T_1 = 0.8$ ,  $T_2 = 0.6$  and  $t_{w1} = 1000$  MCS are presented by solid circles in Fig. 3(a). They are extracted from the replica overlap function eq.(1.1) which is obtained by averaging over several thousands samples with  $L_s = 32$ .

Clearly,  $R_{[T_2, T_1]}(t; t_{w1})$  does grow continuously without any noticeable decrease by the  $T$ -shift. This implies that, just after the  $T$ -shift, the system looks as if it has aged isothermally at  $T = T_2$  for a period of the effective waiting time  $t_{w1}^{(\text{eff})}$  defined in eq.(2.12). Indeed, when  $R_{[T_2, T_1]}(t; t_{w1})$  at  $t > t_{w1}$  is plotted against  $\tilde{t} = t_{w1}^{(\text{eff})} + t_2$  (open triangles in the figure), it almost lies on the isothermal aging curve  $R_{T_2}(t)$ , i.e., the two curves are related as

$$R_{[T_2, T_1]}(t; t_{w1}) \simeq R_{T_2}(t_2 + t_{w1}^{(\text{eff})}), \quad \text{at } t_2 \gtrsim 0. \quad (3.1)$$

Here, a value of  $t_{w1}^{(\text{eff})}$  ( $\simeq 6230$ ) has been chosen so as to obtain a good collapse of the two curves at time range  $t_2 \gtrsim t_{w1}^{(\text{eff})}$ . The chosen value turns out to satisfy eq.(2.12) combined with eqs.(1.2) and (1.3).

As shown in Fig. 3(b),  $R_{[T_2, T_1]}(t; t_{w1})$  in a positive  $T$ -shift protocol is also described by eq.(3.1), but with  $t_{w1}^{(\text{eff})}$  ( $\simeq 1400$ )  $< t_{w1}$  ( $= 10^4$ ) in this case. The continuous growth of domains in the  $T$ -shift process, either a negative or positive one, is one of the most important results observed in the present simulation.

### 3.3 Evolution of energy — Transient and isothermal regimes

In Fig. 4(a) we present the time evolution of energy per spin,  $e_{[T_2, T_1]}(t; t_{w1})$ , in the same negative  $T$ -shift process as shown in Fig. 3(a). The original data drawn by the solid circles quickly deviate from the isothermal aging curve,  $e_{T_1}(t)$ , just after the  $T$ -shift at  $t = t_{w1}$ , and then slowly crossover to  $e_{T_2}(t)$  from below at longer times. As drawn by the open triangles in the figure, the part of  $e_{[T_2, T_1]}(t; t_{w1})$  after the crossover can be laid upon  $e_{T_2}(t)$  if it is shifted rightwards properly, i.e., the two curves are related as

$$e_{[T_2, T_1]}(t; t_{w1}) \simeq e_{T_2}(t_2 + t_{w1}^{(\text{eff})}) \quad \text{at } t_2 \gtrsim t_{w1}^{(\text{eff})}, \quad (3.2)$$

with the same  $t_{w1}^{(\text{eff})}$  as the one determined before through  $R_{[T_2, T_1]}(t; t_{w1})$ . Notice that the shifted  $e_{[T_2, T_1]}(t; t_{w1})$  approaches  $e_{T_2}(t)$  from above.

In the positive  $T$ -shift process,  $e_{[T_2, T_1]}(t; t_{w1})$  behaves similarly and eq.(3.2) also holds as shown in Fig. 4(b). In this case the original (shifted)  $e_{[T_2, T_1]}(t; t_{w1})$  merges into  $e_{T_2}(t)$  from above (below).

From inspection of Figs. 3 and 4 we may divide the aging process after the  $T$ -shift into the following three regimes.

#### 1) Quasi-reversal regime ( $t_2 \leq t_{\text{rev}} \simeq 1$ )

Each spin responds individually to changes in its lo-

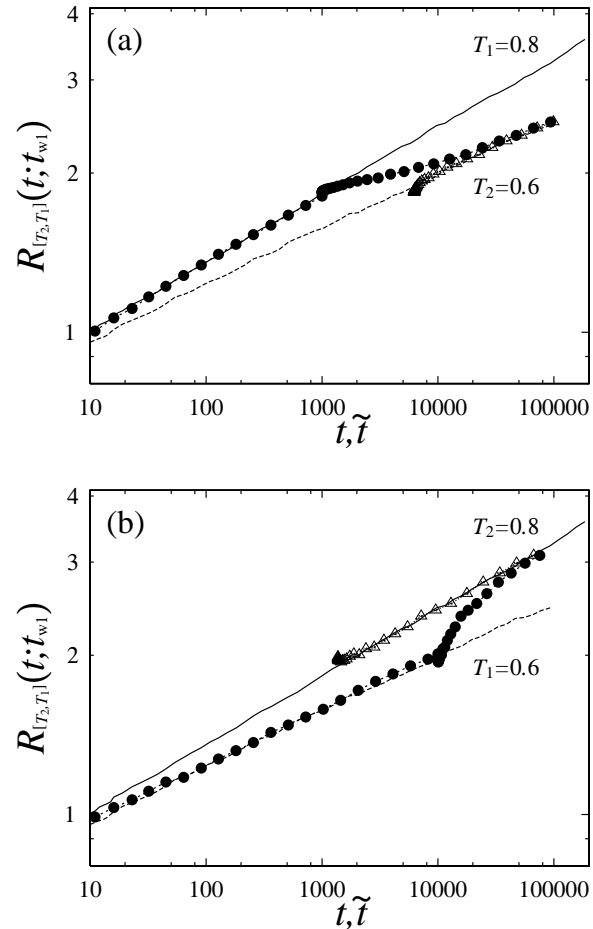


Fig. 3. (a) Growth of  $R_{[T_2, T_1]}(t; t_{w1})$  in a negative  $T$ -shift process with  $T_1 = 0.8$ ,  $T_2 = 0.6$  and  $t_{w1} = 1000$  MCS (solid circles). The solid and broken lines are the isothermal aging curves  $R_{T_1}(t)$  and  $R_{T_2}(t)$ , respectively. The open triangles represent  $R_{[T_2, T_1]}(t; t_{w1})$  plotted against  $\tilde{t} = t_2 + t_{w1}^{(\text{eff})}$  where  $t_2 = t - t_{w1}$  and  $t_{w1}^{(\text{eff})} = 6230$ . (b)  $R_{[T_2, T_1]}(t; t_{w1})$  in a positive  $T$ -shift process with  $T_1 = 0.6$ ,  $T_2 = 0.8$  and  $t_{w1} = 10000$  MCS. The symbols and curves are the same as those in (a) but with  $t_{w1}^{(\text{eff})} = 1400$ .

cal Boltzmann weights. This gives rise to a relatively large change in  $e_{[T_2, T_1]}(t; t_{w1})$  in the first MC step after the  $T$ -shift. The process is expected almost reversible, though we have not explicitly confirmed it.

#### 2) Transient regime ( $t_{\text{rev}} \lesssim t_2 \lesssim t_{w1}^{(\text{eff})}$ )

Judging from the behaviour of  $R_{[T_2, T_1]}(t; t_{w1})$ , eq.(3.1), we may regard that the system has aged roughly for  $t_{w1}^{(\text{eff})}$  at  $T = T_2$  already at around  $t_2 \sim t_{\text{rev}}$ . Actually,  $e_{[T_2, T_1]}(t; t_{w1})$  is significantly smaller (larger) than  $e_{T_2}(t)$  at  $t \gtrsim t_{w1}$  in the negative (positive)  $T$ -shift process.

Another interesting comparison is between  $e_{[T_2, T_1]}(t; t_{w1})$  as a function of  $t_2$  and  $e_{T_2}(t - t_{w1}^{(\text{eff})})$  which is shown in the insets of Fig. 4. Now the former is larger (smaller) than the latter in the negative (positive)  $T$ -shift process, and it relaxes to the latter slowly, at least not exponentially. Within our scenario introduced in §2.3, these can be explained qualitatively as follows. Just after the negative

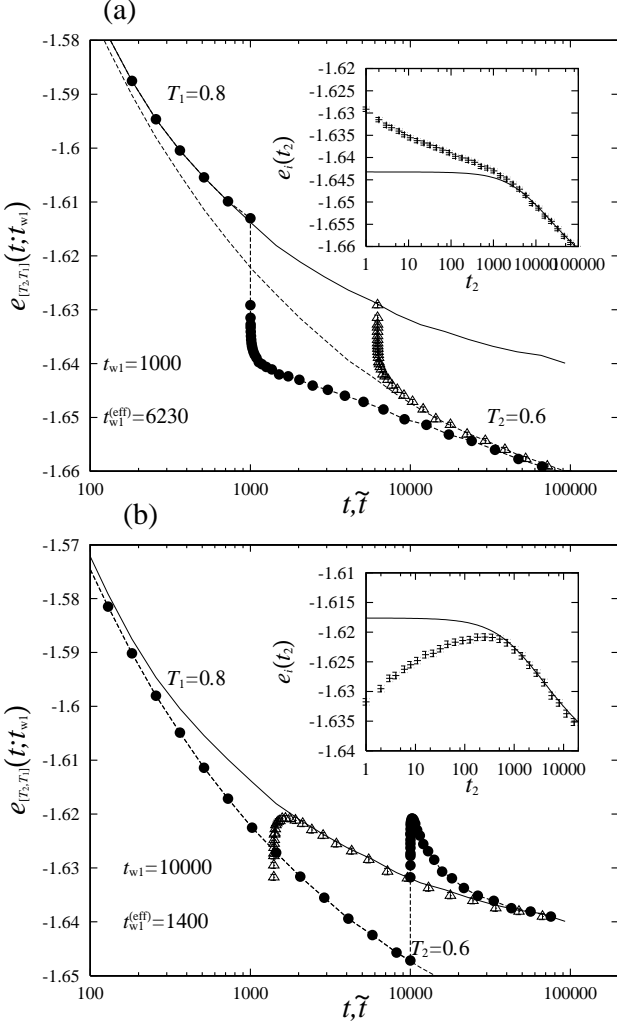


Fig. 4. Time evolution of the energy per density,  $e_{[T_2, T_1]}(t; t_{w1})$ , in the same (a) negative and (b) positive  $T$ -shift protocols as in Fig. 3. The symbols and curves represent  $e_{[T_2, T_1]}(t; t_{w1})$  and  $e_T(t)$  in replacement of  $R_{[T_2, T_1]}(t; t_{w1})$  and  $R_T(t)$ , respectively. In the insets of both figures  $e_{[T_2, T_1]}(t; t_{w1})$  as a function of  $t_2$  and  $e_{T_2}(t - t_{w1}^{(eff)})$  are shown by the data points and the curve, respectively.

(positive)  $T$ -shift, the population of active droplets within the domain is larger (smaller) than in equilibrium at  $T_2$ . Thus the energy density decreases (increases) toward the isothermal curves.

### 3) Isothermal regime ( $t_2 \gtrsim t_{w1}^{(eff)}$ )

In this regime time evolution of the system is nothing but isothermal aging at  $T = T_2$ . The result eq.(3.2) combined with eq.(3.1) means that the mean domain size and the energy density are related by the scaling relation eq.(2.6). The latter implies that relaxation of the energy density in this regime is due to the coarsening of domain walls.

The existence of isothermal regime 3), to which the system crossovers from regime 2) at around  $t_2 \sim t_{w1}^{(eff)}$ , is another important aspect of the aging dynamics observed by the present simulation. It is certainly a consequence of the persistence of domains through the  $T$ -shift process described before, and can be regarded as one of the memory effects. An interesting question is if the phenomena

in transient regime 2) are related with the rejuvenation, or chaos effect observed experimentally.

### 3.4 Spin auto-correlation function

We define the spin auto-correlation function in the  $T$ -shift process as

$$C_{[T_2, T_1]}(\tau; t_{w2}, t_{w1}) = \overline{\langle S_i(\tau + t_{w1} + t_{w2})S_i(t_{w1} + t_{w2}) \rangle}. \quad (3.3)$$

and measure relaxation of

$$\tilde{\chi}_{[T_2, T_1]}(\tau; t; t_{w1}) \equiv \frac{1}{T} [1 - C_{[T_2, T_1]}(\tau; t_2, t_{w1})] \quad (3.4)$$

with increasing  $t_2$  after the  $T$ -shift. At each measurement, a fixed value of the time separation  $\tau$  is chosen as a parameter.

We naively expect that the FDT holds for time regime  $\tau < t_{w2}$  as in the case of isothermal aging (see eq.(2.11)). If it is the case the above  $\tilde{\chi}_{[T_2, T_1]}(\tau; t; t_{w1})$  is identical to the ZFC susceptibility. In experiments, relaxation of the out-of-phase component of the ac susceptibility with a fixed frequency, say  $\omega$ , is most frequently measured also in the  $T$ -shift protocol. It has been numerically ascertained in II that the relaxation of the ac susceptibility at a fixed frequency  $\omega$  is very similar to that of the ZFC susceptibility with a fixed  $\tau = 2\pi/\omega \equiv \tau_\omega$ . Thus we regard  $\tilde{\chi}_{[T_2, T_1]}(\tau_\omega; t; t_{w1})$  as essentially equivalent to the ac susceptibility measured in experiments.

The function with  $t_{w2} = 0$ , denoted by  $C_{[T_2, T_1]}(\tau; 0, t_{w1})$ , was examined in our previous work<sup>18)</sup> hereafter referred to as III. We found that at  $\tau \ll t_{w1}^{(eff)}$  it follows similar scaling forms to those for  $C_T(\tau; t_w)$  in isothermal aging described in §2.1 if the factor  $L_T(\tau)/R_T(t_w)$  in eq.(2.10) is replaced by  $L_{[T_2, T_1]}(\tau; t_{w1})/R_{T_1}(t_{w1})$ . Here  $L_{[T_2, T_1]}(\tau; t_{w1})$  is a mean size of the droplet excitations, or quasi-domains, which are in local equilibrium at the new temperature  $T_2$  within time scale  $\tau$  after the  $T$ -shift.

In Fig. 5 we show typical results of  $\tilde{\chi}_{[T_2, T_1]}(\tau_\omega; t; t_{w1})$  simulated for a fixed  $\tau_\omega$  (= 32). Their behaviours are rather similar to those of  $e_{[T_2, T_1]}(t; t_{w1})$  shown in Fig. 4. Just after the  $T$ -shift, it rapidly decreases (increases) and then relaxes slowly to the isothermal curve  $\tilde{\chi}_{T_2}(\tau_\omega; t)$  from below (above) for  $\Delta T < 0$  ( $> 0$ ). Furthermore, it also satisfies a relation similar to eq.(3.2): when the part of its curve at  $t_2 > 0$  is plotted against  $\tilde{t} = t_2 + t_{w1}^{(eff)}$  it now relaxes to the isothermal curve from above (below),

$$\tilde{\chi}_{[T_2, T_1]}(\tau_\omega; t; t_{w1}) \simeq \tilde{\chi}_{T_2}(\tau_\omega; t_2 + t_{w1}^{(eff)}) \quad \text{at } t_2 \gtrsim t_{w1}^{(eff)}. \quad (3.5)$$

Here, a value of  $t_{w1}^{(eff)}$  ( $\simeq 824$ ) has been chosen so as to obtain a good collapse of the two curves at the time range  $t_2 \gtrsim t_{w1}^{(eff)}$ . The resultant  $t_{w1}^{(eff)}$  is again consistent with eq.(2.12) combined with eqs.(1.2) and (1.3) obtained in I.

The above feature in isothermal regime 3),  $t_2 \gtrsim t_{w1}^{(eff)}$ , means that there the mean domain size and the correlation function are related by the scaling relations of eqs.(2.8), (2.9) and (2.10). Thus relaxation of  $\tilde{\chi}_{[T_2, T_1]}(\tau_\omega; t; t_{w1})$  in this regime is due to increase of the effective stiffness due to the coarsening of domain walls.

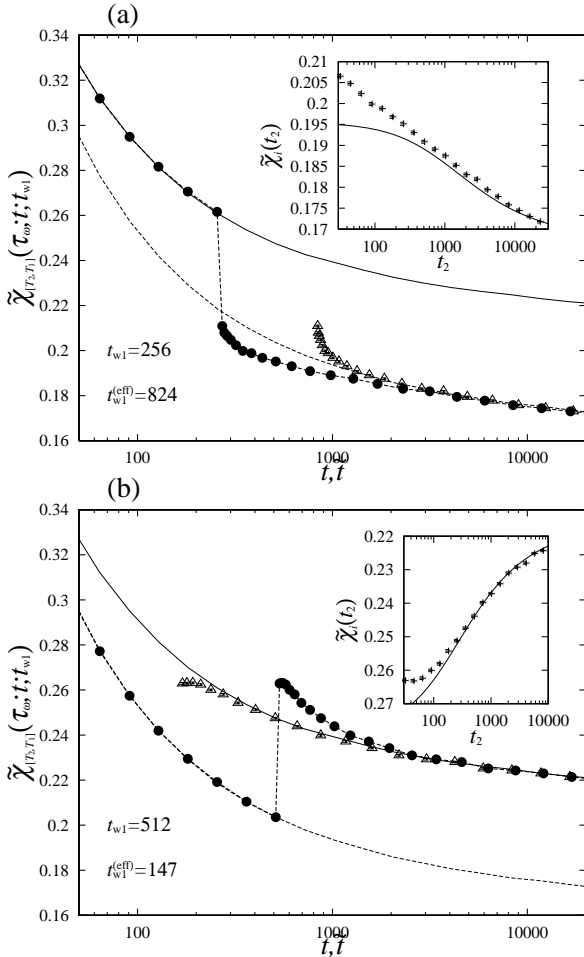


Fig. 5.  $\tilde{\chi}_{[T_2, T_1]}(\tau_\omega; t; t_{w1})$  in a negative  $T$ -shift with  $T_1 = 0.8$ ,  $T_2 = 0.6$  (a) and in a positive  $T$ -shift with  $T_1 = 0.6$ ,  $T_2 = 0.8$  (b). The symbols and curves, including those in the insets, represent  $\tilde{\chi}_{[T_2, T_1]}(\tau_\omega; t; t_{w1})$  and  $\tilde{\chi}_T(\tau_\omega; t)$  in replacement of  $e_{[T_2, T_1]}(t; t_{w1})$  and  $e_T(t)$  in Fig. 4), respectively. The values of  $t_{w1}$  and  $t_{w1}^{(\text{eff})}$  are denoted in each figure.

is considered to reflect nature associated with quasi-domains. Let us here focus on the negative  $T$ -shift shown in Fig. 5(a). As pointed out just above,  $\tilde{\chi}_{[T_2, T_1]}(\tau_\omega; t; t_{w1})$  is definitely smaller than  $\tilde{\chi}_{T_2}(\tau_\omega; t)$  at  $t \gtrsim t_{w1}$ . This is different from the rejuvenation, or chaos effect observed in experiments if it means that the system after the  $T$ -shift is younger than  $t_{w1}$  as for an age in isothermal aging at  $T = T_2$ , i.e.,  $\tilde{\chi}_{[T_2, T_1]}(\tau_\omega; t; t_{w1})$  as a function of  $\tilde{t}$  with  $t_{w1}^{(\text{eff})}$  smaller than  $t_{w1}$  coincides with  $\tilde{\chi}_{T_2}(\tau_\omega; t)$  at  $t_2 \gtrsim t_{\text{rev}}$ .<sup>25)</sup> It may suggest that overlap length  $l_{\Delta T}$  introduced by the droplet theory and expressed as eq.(2.13) in §2.3, if it exists in the present SG model, should be larger than  $R_{T_1}(t_{w1})$  observed in the present simulation.

Let us then compare  $\tilde{\chi}_{[T_2, T_1]}(\tau_\omega; t; t_{w1})$  as a function of  $t_2$  with  $\tilde{\chi}_{T_2}(\tau_\omega; t - t_{w1}^{(\text{eff})})$ . The two curves are shown in the inset of Fig. 5(a). Interestingly, the former is larger than the latter and the excessive part decays very slowly. This feature in transient regime 2) may be explained within the scenario sketched in §2.3 as the following. After  $t_{w2}$  from the  $T$ -shift, there remains excessive population of droplets of length scales larger than the size of the quasi-domain  $L_{[T_2, T_1]}(t_2, t_{w1})$ . The excessive population

is proportional to  $\Delta T = T_2 - T_1$ . The boundary of the latter droplets may act as frozen-in domain walls and reduces the effective stiffness of droplets smaller than  $L_{[T_2, T_1]}(t_2, t_{w1})$  just as in the case of the domain walls which separates different pure states.<sup>17, 13)</sup> This yields the extra contribution, which is proportional to  $\Delta T$ , to the relaxation. The scaling analysis on the excessive part in terms of  $L_{[T_2, T_1]}(t_2, t_{w1})$  and  $R_{[T_2, T_1]}(t; t_{w1})$  is now under investigation.

### 3.5 $T$ -cycling process

A  $T$ -cycling process is a combination of two  $T$ -shift processes with the same  $|\Delta T|$  but with opposite signs. At a time  $t_2 = t_{w2}$  after the  $T$ -shift from  $T_1$  to  $T_2$  the temperature is turned back to  $T_1$ , and the subsequent relaxation is observed. When  $t_{w2} \gg t_{w1}^{(\text{eff})}$ , the  $T$ -change back to  $T_1$  is from an isothermally aged state at  $T_2$ , as shown in Fig. 6(a). In this negative  $T$ -cycling process ( $T_2 < T_1$ ), the approximated ac susceptibility at  $t = t_3 + t_{w2} + t_{w1}$ , now denoted simply by  $\tilde{\chi}_{T(t)}(\tau_\omega; t)$ , merges into the isothermal curve  $\tilde{\chi}_{T_1}(\tau_\omega; t)$  from below when the former is plotted against  $\tilde{t} = t_3 + t_{w2}^{(\text{eff})}$ . Here  $t_{w2}^{(\text{eff})}$  is the effective waiting time given by  $t_{w2}^{z(T_1)/z(T_2)}$  (since  $t_{w2} \gg t_{w1}^{(\text{eff})}$  in this case). In the case that  $t_{w2}$  is small enough, we obtain a similar behaviour but with  $t_{w2}^{(\text{eff})} \simeq t_{w1}$  (not shown). This means that aging at  $T_2$  does not contribute at all to aging at  $T_1$ . This is nothing but the memory effect and has been observed by many experiments.<sup>1, 19, 25)</sup>

In a positive  $T$ -cycling process with  $T_2 > T_1$  shown in Fig. 6(b), our simulated data still exhibit the memory effect in the sense that the curve at  $t_3 > 0$  lies on the isothermal curve of  $T_1$  if it is shifted by a proper amount, i.e.,  $t_{w2}^{(\text{eff})}$  which depends not only  $t_{w2}$  but also on  $t_{w1}$ . This type of memory retained over a positive  $T$ -cycling has been indeed observed in the ferromagnetic fine particle system.<sup>25)</sup>

### 3.6 Continuous $T$ -change with an intermittent stop

We have also performed simulations on a continuous  $T$ -change with an intermittent stop. Following the experimental protocol,<sup>22)</sup> we cool a system by a constant rate from above  $T_c$  to below  $T_c$  with an intermittent stop at a certain temperature  $T_1$  below  $T_c$ , restart the cooling, and then heat it back by the same rate as in the cooling. A typical result is shown in Fig. 7. In this analysis  $\tilde{\chi}_{T(t)}(\tau_\omega; t)$  has been directly measured as the response to an ac field  $h(t) = h_0 \sin(\omega t)$  with  $h_0 = 0.3$  and  $2\pi/\omega = 160$  (MCS).

At the intermittent stop at  $T_1$ ,  $\chi''_{T(t)}(\omega; t)$  relaxes downward and deviates from the reference curve of cooling. After restarting the cooling,  $\chi''_{T(t)}(\omega; t)$  is seen to merge into the reference curve. It appears that the long time aging at  $T_1$  does not affect subsequent cooling at temperatures lower than  $T_1$  by a certain amount. Here we call this phenomenon a rejuvenation-like effect, since  $\chi''_{T(t)}(\omega; t)$  merges with the reference curve but without a strong vertical increase in contrast to the rejuvenation seen in the experiment.<sup>22)</sup>

When the system is heated back from the lowest tem-

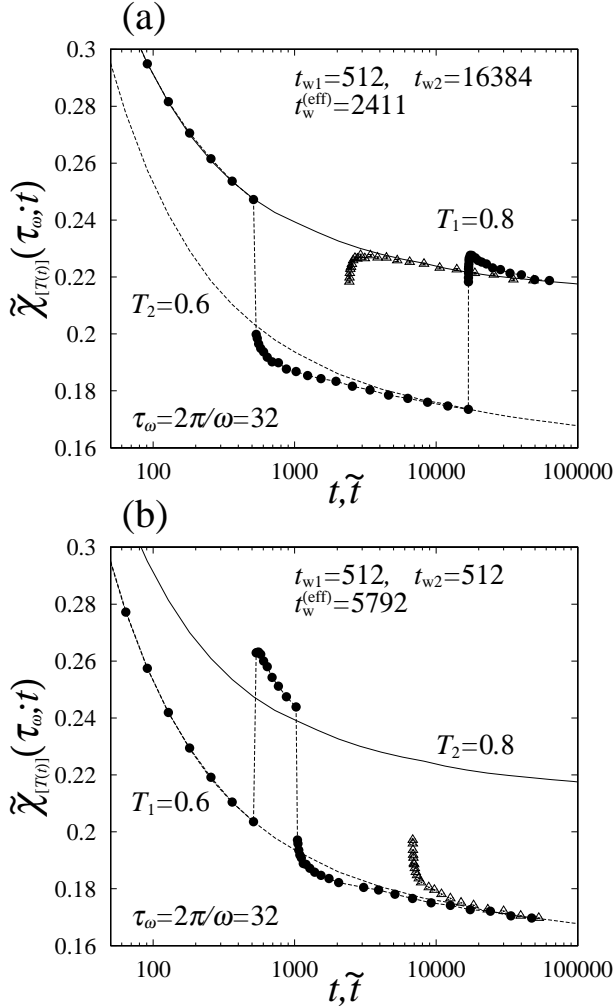


Fig. 6.  $\tilde{\chi}_{T(t)}(\tau_\omega; t)$  in a negative  $T$ -cycling with  $T_1 = T_3 = 0.8$ ,  $T_2 = 0.6$  (a) and in a positive  $T$ -cycling with  $T_1 = T_3 = 0.6$ ,  $T_2 = 0.8$  (b). The symbols and lines are the same as those in Fig. 5 but with  $\tilde{t} = t_3 + t_w^{(\text{eff})}$ .

perature of cooling process,  $\chi''_{T(t)}(\omega; t)$  exhibits a dip at around  $T = T_1$ , though it is rather shallow. This means that the memory imprinted by the long time aging at  $T_1$  in the cooling process, in fact, has not been erased until the system comes back to  $T_1$  from the lower temperatures. To conclude the present SG model exhibits the rejuvenation-like and memory effects within a time-window of the present simulation.

#### §4. Discussions

We have studied aging phenomena in various  $T$ -change protocols on the 3D Gaussian Ising SG model by Monte Carlo simulations. In particular, we have argued that, in a  $T$ -shift protocol, slow aging dynamics after the  $T$ -change from  $T_1$  to  $T_2$  at  $t_2 = 0$  consists of two regimes: transient ( $t_2 \lesssim t_{w1}^{(\text{eff})}$ ) and isothermal ( $t_2 \gtrsim t_{w1}^{(\text{eff})}$ ) regimes, where  $t_{w1}^{(\text{eff})}$  is the effective waiting time specified by eq.(2.12). In the transient regime, re-distribution of thermal weights, from those at  $T_1$  to  $T_2$ , of droplet excitations with the characteristic length scale  $L_{[T_2, T_1]}(t_2, t_{w1})$  is taking place within each domain of the mean size  $R_{[T_2, T_1]}(t; t_{w1})$ . We called the length

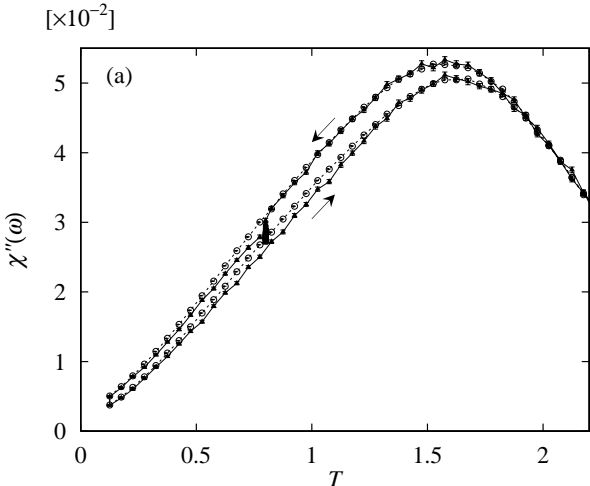


Fig. 7.  $\tilde{\chi}_{T(t)}(\tau_\omega; t)$  in a continuous  $T$ -change with an intermittent stop. We cool and re-heat the system continuously with a constant rate of  $J/3200$  per MCS from  $T = 3.0$  to  $T = 0.1$ . The open circles represent the reference curves in cooling (upper curve) and re-heating (lower curve) protocols. The solid circles represent the same protocol except for an intermittent stop in cooling at  $T_1 = 0.8$  for 32000 MCS.

scale  $L_{[T_2, T_1]}(t_2, t_{w1})$  as the size of quasi-domains.

Suppose, in a negative  $T$ -shift process, we further decrease temperature to  $T_3$  ( $< T_2$ ) at  $t_2 = t_{w2}$  ( $\ll t_{w1}^{(\text{eff})}$ ) and wait a certain period. Then there appear now quasi-domains locally equilibrated to  $T_3$  within each quasi-domain of  $T_2$ . Because of the wide separation of time scales at different length scales emphasized in §2.1, a nest (or hierarchy) of quasi-domains can be realized dynamically when the system is cooled step-wise, or continuously. At low temperatures the ac field can only excite droplets of the size  $L_T(1/\omega)$  corresponding to the frequency  $\omega$ . If the size is small enough, a new contribution to the ac response will appear every time a new frozen-in domain wall appears associated with the quasi-domain due to a step of cooling. This is our interpretation of the rejuvenation-like effect seen in Fig. 7. Its observation then crucially depends on time and length scales by which one looks at the system. It is the easier to be observed, the shorter and smaller are the time and length scales.

By means of our scenario the memory effect is rather easy to be understood. For example, the continuous  $T$ -change protocol shown in Fig. 7 is interpreted as follows. When the system is re-heated from the lowest temperature, the hierarchical structure of quasi-domains is erased from the lower levels. When the temperature comes back to  $T_1$ , the large domains imprinted at the intermittent stop in the cooling process reappear and govern the response of the system, which causes the memory effect in this protocol. According to our scenario, a memory imprinted by aging at a certain temperature  $T_1$  is erased when the system is aged at different temperature, say  $T_d$ , for such a long period that the mean size of quasi-domains of  $T_d$  catches up the domains imprinted at  $T_1$ , as what happens in regime 3) of the  $T$ -shift protocol. Even in that case, the memory of the previous thermal

history is kept in the effective waiting time, i.e., the system looks more aged than the period that it is actually aged at  $T = T_d$  (see eq.(3.5)).

Let us now compare our simulated results with experimental observations. As pointed out already in §1, in the ferromagnetic fine particles system (FFPS), whose aging dynamics has been recently studied by Mamiya *et al.*,<sup>25)</sup> the microscopic time,  $\tau_{\text{mic}}$ , required for a magnetic moment of each fine particle to flip is of the order of  $10^{-3}$  sec.<sup>26)</sup> Therefore the time window of their observation,  $1 \sim 10^3$  ksec, in unit of  $\tau_{\text{mic}}$  is not much different from that of our MC simulation. It is also noted that in the FFPS each magnetic moment behaves as an Ising spin due to strong magnetic anisotropy.

Indeed in the *T*-shift protocol, Mamiya *et al.* have observed relaxation of  $\chi''_{[T_2, T_1]}(\omega; t; t_{w1})$  which is qualitatively quite similar to our simulated  $\tilde{\chi}_{[T_2, T_1]}(\tau_\omega; t; t_{w1})$  shown in Fig. 5. They have determined amount of the shift of  $\chi''_{[T_2, T_1]}(\omega; t; t_{w1})$ , or  $t_{w1}^{(\text{eff})}$ , by the same method that we have used for analysis of  $\tilde{\chi}_{[T_2, T_1]}(\tau_\omega; t; t_{w1})$  in Fig. 5. The effective waiting time they obtained is written as  $t_{w1}^{(\text{eff})} \simeq 3 \times (t_{w1})^b$  with  $b \simeq 1.0$ . By contrast,  $t_{w1}^{(\text{eff})}$  extracted from our simulation is given by eq.(2.12), which, with making use of eq.(1.2), is reduced to  $t_{w1}^{(\text{eff})} \propto (t_{w1})^b$  with  $b = z(T_2)/z(T_1)$  ( $\simeq 1.11$  (1.25) for  $T_1 = 0.8$  and  $T_2 = 0.7$  (0.6)). Also aging dynamics of the FFPS in the *T*-cycling protocol agrees qualitatively with the results of our simulation. In particular, the effective waiting time  $t_w^{(\text{eff})}$  which depends on  $t_{w1}$  (memory effect) is observed even in the positive *T*-cycling process, though Mamiya *et al.* have claimed that the memory is partially lost because some particles with a larger size than the average are affected by the chaos effect associated with the temperature change.

For ordinary spin glasses with  $\tau_{\text{mic}} \sim 10^{-13}$  sec, there have been only a few experiments, in which  $t_{w1}^{(\text{eff})}$  in the *T*-shift process is systematically studied. Djurberg *et al.*<sup>28)</sup> measured the ZFC magnetization of Cu:Mn 13.5at% spin glass with a fixed  $t_{w1}$  and varying  $\Delta T$ . Via the FDT similar to eq.(2.11) their analysis is directly comparable with our simulation on  $C_{[T_2, T_1]}(\tau; 0, t_{w1})$  in III. The peak position of its relaxation rate with respect to  $\text{Int}$  may be assigned as  $t_{w1}^{(\text{eff})}$  (crossover from regime 2) to (regime 3)). The experimentally observed  $t_{w1}^{(\text{eff})}$  becomes larger (smaller) than  $t_{w1}$  in the positive (negative) *T*-shift, which is qualitatively consistent with eq.(2.12) with monotonic increase of  $1/z(T)$  on  $T$ . Quantitatively, however, the shift observed experimentally is much larger than what is expected from eq.(1.3).

Djurberg *et al.*<sup>28)</sup> furthermore claimed that they observed the chaos effect in *T*-shift processes with  $|\Delta T|$  larger than a certain value. The rejuvenation, or chaos effect in the *T*-shift and *T*-cycling protocols observed in  $\chi''_{T(t)}(\omega; t)$  has been reported for CdCr<sub>1.7</sub>In<sub>0.3</sub>S<sub>4</sub><sup>19, 21)</sup> and Cu:Mn 2at%<sup>20)</sup> spin glasses, as already mentioned in §1. The observed  $\chi''_{T(t)}(\omega; t)$  is claimed<sup>27)</sup> to indicate that the system is literally rejuvenated in the sense described in §3.4. Neither such a chaos effect nor literal rejuvenation have been seen in our present simulations (see also Kisker *et al.*<sup>10)</sup>). At the moment it is not

clear yet whether this discrepancy originates simply from the difference in time scales of the observations, or from something else.

To conclude, we have simulated various *T*-change protocols of aging in the 3D Ising SG model, and have proposed a scenario in terms of domains and quasi-domains: the former ever grow in any aging process in the SG phase and the latter appear within the former or within themselves. The results observed in our simulations are reasonably well interpreted by the scenario. Qualitatively, it is also consistent with many features observed experimentally, particularly, those related to the memory effect. For certain phenomena such as the growth law of  $R_T(t)$ , the consistency is even semi-quantitative. Concerned with the rejuvenation, or chaos effect, however, the scenario may not be applicable, and further studies are required.

### Acknowledgments

We would like to sincerely thank E. Vincent and M. Ocio for their fruitful discussions and for kindly allowing us to use their data on a AgMn spin glass. We also thank H. Mamiya for his helpful discussions on the experiments of his research group. Our thanks are also to J.P. Bouchaud, K. Hukushima and P. Nordblad for their useful discussions. Two of the present authors (T. K. and H. Y.) were supported by Fellowships of Japan Society for the Promotion of Science for Japanese Junior Scientists. This work is supported by a Grant-in-Aid for International Scientific Research Program, "Statistical Physics of Fluctuations in Glassy Systems" (#10044064) and by a Grant-in-Aid for Scientific Research Program (#10640362), from the Ministry of Education, Science and Culture. The present simulation has been performed on FACOM VPP-500/40 at the Supercomputer Center, Institute for Solid State Physics, the University of Tokyo.

- [1] E. Vincent, J. Hammann, M. Ocio, J.P. Bouchaud and L.F. Cugliandolo: in *Proceeding of the Sitges Conference on Glassy Systems*, ed. E. Rubi (Springer, Berlin, 1996).
- [2] P. Nordblad and P. Svendelidh: in *Spin-glasses and random fields*, ed. A. P. Young, (World Scientific, Singapore, 1997).
- [3] M.B. Weissman: in the same book as in Ref. 2.
- [4] J.P. Bouchaud, L.F. Cugliandolo, J. Kurchan and M. Mézard: in the same book as in Ref. 2.
- [5] J.P. Bouchaud: preprint, cond-mat/9910387.
- [6] J.-O. Andersson, J. Mattsson and P. Svedlindh: Phys. Rev. B **49** (1994) 1120.
- [7] H. Rieger: J. Phys. I France **4** (1994) 883.
- [8] H. Rieger: Physica A **224** (1996) 267.
- [9] D.A. Huse: Phys. Rev. B **43** (1991) 8673.
- [10] J. Kisker, L. Santen, M. Schreckenberg and H. Rieger: Phys. Rev. B **53** (1996) 6418.
- [11] E. Marinari, G. Parisi, F. Ricci-Tersenghi and J. J. Ruiz-Lorenzo: J. Phys. A **31** (1998) 2611.
- [12] T. Komori, H. Yoshino and H. Takayama: J. Phys. Soc. Jpn. **68** (1999) 3387.
- [13] T. Komori, H. Yoshino and H. Takayama: to appear in J. Phys. Soc. Jpn. (**69** (2000) No. 4 (cond-mat/9909228)).
- [14] D.S. Fisher and D.A. Huse: Phys. Rev. Lett. **56** (1986) 1601.
- [15] A.J. Bray and M.A. Moore: in *Heidelberg Colloquium in Glassy Dynamics*, ed. by J.L. van Hemmen and I. Morgenstern, Lecture Notes in Physics Vol. 275 (Springer-Verlag, Heidelberg, 1987), p.121.
- [16] D. S. Fisher and D. A. Huse: Phys. Rev. B **38** (1988) 386.

- [17] D. S. Fisher and D. A. Huse: Phys. Rev. B **38** (1988) 373.
- [18] H. Takayama, H. Yoshino and T. Komori: Intern. J. Mod. Phys. C **10** (1999) 1433.
- [19] F. Lefloch, J. Hammann, M. Ocio and E. Vincent: Europhys. Lett. **18** (1992) 647.
- [20] J.O. Andersson, J. Mattsson and P. Nordblad: Phys. Rev. B **48** (1993) 13977.
- [21] E. Vincent, J.-P. Bouchaud, J. Hammann and F. Lefloch: Phil. Mag. B **71** (1995) 489.
- [22] K. Jonason, E. Vincent, J. Hammann, J.-P. Bouchaud, and P. Nordblad: Phys. Rev. Lett. **81** (1998) 3243.
- [23] K. Jonason, P. Nordblad, E. Vincent, J. Hammann and J.P. Bouchaud: cond-mat/9904410, Euro. Phys. J. B in print.
- [24] T. Komori: PhD thesis, University of Tokyo, 1999.
- [25] H. Mamiya, I. Nakatani and T. Furubayashi: Phys. Rev. Lett. **82** (1999) 4332.
- [26] H. Mamiya: private communication.
- [27] E. Vincent: private communication.
- [28] C. Djurberg, K. Jonason and P. Nordblad: Euro. Phys. J. B **10** (1999) 15.
- [29] A. J. Bray and M. A. Moore: J. Phys. C **17** (1984) L463.
- [30] M. Alba, J. Hammann, M. Ocio and Ph. Refregier: J. Appl. Phys. **61** (1987) 3683.
- [31] Ph. Refregier, M. Ocio, J. Hammann and E. Vincent: J. Appl. Phys. **63** (1988) 4343.
- [32] E. Marinari, G. Parisi and J.J. Ruiz-Lorenzo: Phys. Rev. B **58** (1998) 14852.
- [33] Y. G. Joh, R. Orbach, G. G. Wood, J. Hammann and E. Vincent: Phys. Rev. Lett. **82** (1999) 438.
- [34] K. Hukushima, H. Yoshino and H. Takayama: to appear Prog. Theor. Phys. Suppl. (cond-mat/9910414).
- [35] A. J. Bray and M. A. Moore: Phys. Rev. Lett. **58** (1987) 57.